Materials Research Innovations

ISSN: 1432-8917 (Print) 1433-075X (Online) Journal homepage: http://www.tandfonline.com/loi/ymri20

Preparation of zinc layered hydroxide-ferulate and coated zinc layered hydroxide-ferulate nanocomposites for controlled release of ferulic acid

Norhayati Hashim, Sharifah Norain Mohd Sharif, Zuhailimuna Muda, Illyas Md Isa, Noorshida Mohd Ali, Suriani Abu Bakar, Siti Munirah Sidik & Mohd Zobir Hussein

To cite this article: Norhayati Hashim, Sharifah Norain Mohd Sharif, Zuhailimuna Muda, Illyas Md Isa, Noorshida Mohd Ali, Suriani Abu Bakar, Siti Munirah Sidik & Mohd Zobir Hussein (2018): Preparation of zinc layered hydroxide-ferulate and coated zinc layered hydroxide-ferulate nanocomposites for controlled release of ferulic acid, Materials Research Innovations, DOI: 10.1080/14328917.2018.1444696

To link to this article: https://doi.org/10.1080/14328917.2018.1444696

Published online: 02 Mar 2018.

MATERIALS RESEARCH INNOVATIONS, 2018
https://doi.org/10.1080/14328917.2018.1444696

Taylor & Francis
Taylor & Francis Group

Preparation of zinc layered hydroxide-ferulate and coated zinc layered hydroxide-ferulate nanocomposites for controlled release of ferulic acid

Norhayati Hashim[a,b], Sharifah Norain Mohd Sharif[a], Zuhailimuna Muda[a], Illyas Md Isa[a,b], Noorshida Mohd Ali[a], Suriani Abu Bakar[b,c], Siti Munirah Sidik[a] and Mohd Zobir Hussein[d]

[a]Faculty of Science and Mathematics, Department of Chemistry, Universiti Pendidikan Sultan Idris, Tanjong Malim, Malaysia; [b]Nanotechnology Research Centre, Faculty of Science and Mathematics, Universiti Pendidikan Sultan Idris, Tanjong Malim, Malaysia; [c]Faculty of Science and Mathematics, Department of Physics, Universiti Pendidikan Sultan Idris, Tanjong Malim, Malaysia; [d]Materials Synthesis and Characterization Laboratory, Institute of Advanced Technology, Universiti Putra Malaysia, Serdang, Malaysia

ABSTRACT

Ferulic acid (FA) was intercalated into zinc layered hydroxide (ZLH) to form a new nanocomposite, namely zinc layered hydroxide-ferulate (ZLH-FA) and was further coated by surfactants sodium dodecyl sulfate (SDS) and polysorbate 80 (Tween-80). XRD patterns of the ZLH-FA nanocomposite obtained reveals a crystalline structure with basal spacing of 26·9 Å. The XRD pattern of the coated nanocomposite showed similar peaks to the ZLH-FA nanocomposite. The loading of FA in the nanocomposite was estimated to be 56·82% (w/w), and its thermal stability was markedly enhanced compare to its free counterpart. A controlled release study showed that the FA was release was slower from interlayer of ZLH-FA/SDS and ZLH-FA/Tween-80 nanocomposites compared to the ZLH-FA nanocomposite. The mechanism of release follow the pseudo-second order kinetics model for all nanocomposites. Results from this study highlight the potential of these nanocomposites for controlled release formulation of FA drug anion.

ARTICLE HISTORY
Received 21 October 2017
Accepted 18 February 2018

KEYWORDS
Nanocomposite; zinc layered hydroxide; ferulic acid; direct reaction method; controlled release

Introduction

Layered metal hydroxides can be categorized into layered double hydroxide (LDH) and layered hydroxide salt (LHS) structures. Zinc layered hydroxide (ZLH) is a type of LHS, having the general formula of $M^{2+}(OH)_{2-x}(A^{m-})^{x/m}.nH_2O$, where M^{2+} in this case is the metal cation Zn^{2+} and A^{m-} is the counter ion [1]. Similar to other LDH phases, ZLH undergoes anion-exchange reactions by substituting negatively charged organic molecules for the exchangeable interlayer anion in the ZLH phase to form a layered nanocomposite [2]. The 2D layered inorganic material is composed of layers with octahedral coordinated zinc cations, in which a quarter of them are displaced out of layer, leaving an empty octahedral site which forms cationic centres tetrahedrally coordinated to the top and bottom of the octahedral sheet [3]. In recent years, there has been extensive research on the use of ZLH as drug carriers [4,5], slow release herbicides [6], flame retardants [7] and anti-corrosion agents [8].

Most drugs are not water soluble, leading to ineffective dose delivery and unwanted side effects. Additionally, there are many cases where conventional drug administration methods do not provide satisfactory pharmacokinetic profiles because the drug concentration rapidly falls below the desired levels [9]. Furthermore, the rapid release of drugs leads to many issues due to the uncontrollable release rate. A fluctuation in drug levels in the blood stream and other target organs, enzymatic degradation, poor water solubility and the necessity of high drug doses which arise from these conventional therapeutic systems causes many adverse effects [10]. Therefore, there is a focus on development of effective reservoirs, such as controlled-release drug delivery systems, which offer many pharmaceutical benefits by retaining drug bioactivity, reducing side effects, prolonging duration time, balancing drug concentrations within a desired range and facilitating drug delivery to patients [11].

The term 'drug delivery system' (DDS) refers to the technology utilised to present a drug to the desired body sites for drug release and absorption. Controlled release systems are methods that can achieve therapeutically effective concentrations of drugs in systemic circulation over an extended period of time and with better patient compliance [12]. One of the possibilities for delivering drugs to the body is by the employment of inorganic particles. The versatility of inorganic particles, such as wide availability, good biocompatibility and rich functionality, have garnered considerable attention as a DDS [13]. In addition, nanoparticle-based DDS can slowly release the carried drugs in order to maintain concentrations at the desired levels for an extended period of time [14].

Having similar characteristics to LDH, ZLH have also emerged as promising drug delivery carriers because of several notable properties, such as ease of preparation, low cost, good biocompatibility, low cytotoxicity and full protection of the drugs loaded [15]. ZLH have been widely applied for the delivery of different pharmaceutical drugs, such as cetirizine [16], cinnamic acid [17], protocatechuic acid [18], para-aminosalicylic acid [19], hippuric acid [5] and ciprofloxacin [20].

However, drug delivery may be hindered due to poor water solubilization, agglomeration, inadequate targeted delivery, minimal thermal stability and surface charges of LDH [10]. These problems will likely be overcome through surface

CONTACT Norhayati Hashim norhayati.hashim@fsmt.upsi.edu.my

modifications which can alter particle size, size distribution, particle morphology, surface chemistry, surface hydrophobicity, zeta potential and drug encapsulation efficiency. A suitable surface coating material is essential in order to achieve success in the controlled release formulation of drugs. A number of materials have been used as coating materials in the past such as Tween-80 [21], poly(ethylene) glycol (PEG) [22], dextran [23], Eudragit®L 100 [24], sodium oleate [25] and chitosan [26]. These coatings are sometimes used as targeting materials, helping in nanoparticle delivery to specific areas, increasing the stability or decreasing the toxicity potentials.

Ferulic acid (FA) is a drug that is a phenolic acid and exhibits a wide range of therapeutic effects against various diseases, including cancer, diabetes and cardiovascular and neurodegenerative diseases. It has also been attracting much interest due to its biomedical effects, such as antioxidant, antimicrobial, anti-inflammatory, antiallergic, anticarcinogenic, antithrombotic, antiviral, hepatoprotective and vasodilatory properties [27,28]. To the best of our knowledge, the use of ZLH as a matrix, particularly in DDS, is very limited and needs to be explored.

In this study, FA has been intercalated into the interlayer of ZLH to produce a ZLH-FA nanocomposite using a direct reaction method which is relatively simple, environmentally friendly and economical, as it includes fewer chemicals and steps. The ZLH-FA nanocomposite was further coated with surfactants, sodium dodecyl sulphate (SDS) and Tween-80, to form new coated nanocomposites, namely ZLH-FA/SDS and ZLH-FA/Tween-80, in order to enhance its properties and effectiveness as the DDS. The structure and morphology of synthesised nanocomposites were studied by powder X-ray diffraction (PXRD), Fourier-transform infrared spectroscopy (FTIR), CHNS elemental analysis, inductively coupled plasma optical emission spectroscopy (ICP/OES), Thermal Gravimetric Analysis/Derivative Thermogravimetric Analysis (TGA/DTG), field emission scanning electron microscopy (FESEM) and transmission electron microscopy (TEM). Based on previous reports, intercalation of FA into ZLH by a direct reaction method and further coating of the nanocomposite by the previously mentioned surfactants has not yet been reported. Phosphate buffer solutions with two different pH values were used to study the controlled release of FA from the interlayers of nanocomposites. In addition, the release behaviour of FA was determined using five kinetic orders.

Experimental

Materials

Zinc oxide (ZnO) and FA were purchased from Acros Organic, SDS from Sigma Aldrich and Tween-80 from Fisher Scientific. All chemicals were of analytical grade and used without further purification. Deionized water was used in the synthesis of nanocomposites and for the preparation of solutions.

Synthesis of ZLH-FA nanocomposites

ZLH-FA nanocomposites were synthesised using ZnO as starting material, by a direct method similar to those previously described [5,16,29]. Solution of FA (0·05 M) was prepared by dissolving the required amount of FA in 50 ml of 99·8% methanol. 0·50 g of ZnO powder was suspended in 20 ml of water. Then, the prepared of FA solution was added into the ZnO suspension and magnetically stirred for 2½ hours at room temperature. The resulting slurry was aged in an oil bath shaker at 70 °C for 24 h [30]. Next, the precipitate was centrifuged, thoroughly washed by deionized water and dried in an oven at 60 °C overnight. It was ground and kept in a sample bottle for further use and characterisation.

Synthesis of ZLH-FA/SDS and ZLH-FA/Tween-80 nanocomposites

ZLH-FA/SDS and ZLH-FA/Tween-80 nanocomposites were synthesised according to Kura et al. [21] and Kameshima et al. [25]. The ZLH-FA nanocomposite (0·10 g) was added to 0·0025 M of coating solution and magnetically stirred for 18 h at room temperature. The precipitate was centrifuged and dried in an oven over night. It was ground and kept in a sample bottle.

Characterisation

X-ray diffraction patterns were recorded with a Bruker AXS Powder Diffractor using CuK_{α} radiation (λ = 1·5406 Å) at 60 kV and 60 mA, with a scanning rate of 0·025 °s^{-1}. The infrared spectra were recorded in the range of 400–4000 cm^{-1} on a Thermo Nicolet 6700 Fourier Transform Infrared Spectroscope using the KBr pallet method. Thermal analyses were performed using a Perkin Elmer Pyris 1 TGA Thermo Balance with a heating rate of 20 °C min^{-1}. The composition of carbon, hydrogen and nitrogen was analysed using a CHNS instrument (model Thermo Finnigan). Inductively coupled plasma optical emission spectroscopy (model Agilent 720 Axial) was used to determine the percentage of zinc present in the nanocomposite. A field emission scanning electron microscope and transmission electron microscope (Hitachi model SU 8020 UHR) were used to observe the surface morphology and cross-section of the nanocomposites, respectively.

Controlled release study

The controlled release study was performed using an UV-visible spectrophotometer (Agilent Cary 60). The release behaviour of the FA drug from ZLH-FA, ZLH-FA/SDS and ZLH-FA/Tween-80 nanocomposites was studied in a human body-simulated, phosphate buffer solution at pH 4·8 and 7·4 [16,18].The purpose of using phosphate buffer solution with two different pH values was to determine whether the release of FA from the interlayers of the nanocomposite was pH dependent, or not. The phosphate buffer solution contained a number of anions, such as Cl^-, monobasic phosphate $H_2PO_4^-$ and dibasic phosphate HPO_4^{2-}. About 5 mg of nanocomposite was dispersed into a 200 ml buffer solution and stirred continuously. The amount of ferulate released into the solution was measured using a UV–visible spectrophotometer (Agilent Cary 60) at pre-set time intervals (λ_{max} = 321 nm).

Results and discussion

Powder X-ray diffraction

Powder X-ray diffraction (PXRD) was the preliminary technique used to verify the successful intercalation of the anion into the interlayer of ZLH and to identify whether the layered structure was altered, or not, after treatments with the coating materials based on the changes of it basal spacing [31].

Figure 1 shows the XRD patterns of the ZnO, FA and ZLH-FA nanocomposite. PXRD of the pure ZnO revealed that the solid had good crystallinity, with five intense peaks between 30° and 60°, corresponding to the (100), (002), (101), (102) and (110) planes, and in agreement with previous reports [5,16].

As shown in Figure 1, ZLH-FA nanocomposite synthesised using 0·05 M of FA show peaks at a lower 2θ angle which indicated the successful intercalation of the FA drug into the interlayer of ZLH. The appearance of symmetrical, sharp, intense and high intensity diffraction peaks at 2θ angle of 3·4° and 6·8° with basal spacing of 26·9 and 13·1 Å, respectively signifies good crystallinity own by the nanocomposite. Total disappearance of the intense peaks of the ZnO phase indicated that the ZLH-FA nanocomposite was pure phase and the ZnO was completely converted to ZLH [32]. In addition, no crystalline impurities of pure FA were detected in the nanocomposite, thus strongly supporting that 0·05 M of FA is the optimum condition to obtain a well-ordered nano-layered structure with good crystallinity.

The formation of the ZLH-FA nanocomposite by direct reaction of ZnO with FA under aqueous environment is believed to occur through a dissociation-deposition mechanism, as reported by Xingfu et al. [33], Hussein et al. [32], Bang et al. [34] and Mohsin et al. [17]. Equation (1) refers to the first step, which involves the hydrolysis of ZnO in water. When ZnO particles are immersed in water, the surface of ZnO hydrolyses to form a layer of $Zn(OH)_2$. In the presence of acid, the layer of $Zn(OH)_2$ becomes more soluble. Therefore, dissociation of $Zn(OH)_2$ into Zn^{2+} and $2OH^-$ takes place, as shown in Equation (2). Finally, Zn^{2+}, hydroxyl, H_2O and the ferulate ion in the solution react, to generate the layered intercalation compound, as shown in Equation (3). This process is repeated until all of the ZnO phase and $Zn(OH)_2$ phase have completely converted into the layered compound. The mechanism is described in Equations (1)–(3) below:

$$ZnO + H_2O \rightleftharpoons Zn(OH)_2 \quad (1)$$

$$Zn(OH)_2 \rightleftharpoons Zn^{2+} + 2OH^- \quad (2)$$

$$Zn(OH)_2 \rightleftharpoons Zn^{2+} + 2OH^- \quad (3)$$

$$Zn^{2+} + 2OH^- + FA^- + H_2O \rightleftharpoons Zn^{2+}(OH)_{2-x}(FA^-)_x.nH_2O \quad (4)$$

Figure 2 shows the XRD pattern of the ZLH-FA/SDS and ZLH-FA/Tween-80 nanocomposites. As shown in Figure 2, there is not much difference between the ZLH-FA nanocomposite and the associated coated nanocomposites. Both coated nanocomposites, ZLH-FA/SDS and ZLH-FA/Tween-80, showed intense peaks at the lower angle with a basal spacing of 26·6 Å. The basal spacing of the coated nanocomposites was smaller compared to the uncoated nanocomposite due to the slightly different orientation of the FA anion in the interlayers of the ZLH. Based on these results, it shows that the addition of coating materials, SDS and Tween-80, only resulted in absorption of the former on the surface of ZLH and did not affect any phase change in the ZLH-FA nanocomposite.

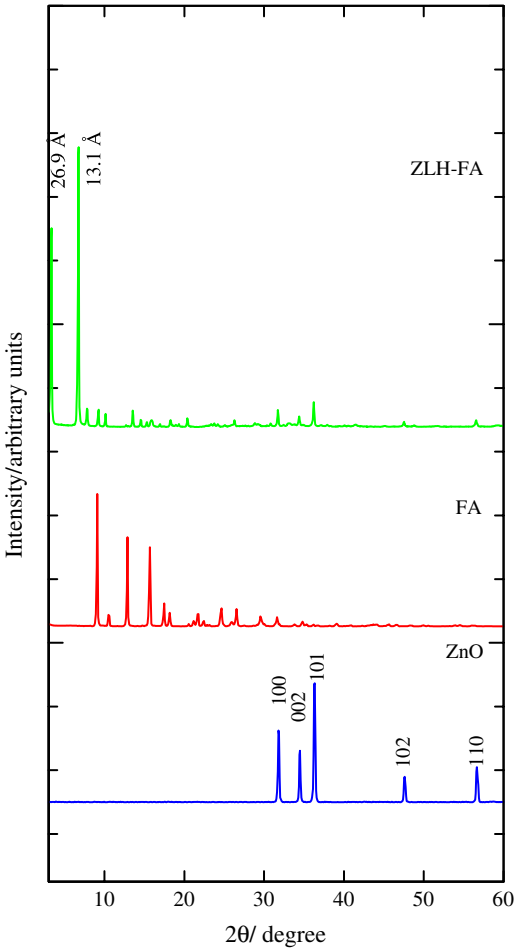

Figure 1. Powder X-ray diffraction patterns of ZnO, FA and ZLH-FA nanocomposites synthesized using 0.05 M FA.

Spatial orientation of intercalated ferulate

The proposed spatial arrangement of the FA within the interlayer region of ZLH is shown in Figure 3. Based on the PXRD data and the 3D molecular size of FA, the calculation obtained using Chem3d Ultra 8.0 software is illustrated in Figure 4. The ZLH was composed of inorganic layers with octahedral coordinated zinc cations, of which a quarter were displaced out of the layer, leaving an empty octahedral site [3]. Using the average basal spacing of 26·9 Å for FA observed by PXRD, and subtracting the thickness of the 4·8 Å brucite layer and 2·6 Å for each zinc tetrahedron [35], the gallery height was calculated to be 16·9 Å.

Considering the observed interlayer spacing from PXRD (16·9 Å), the charge density of the ZLH layers and the approximate dimensions of the FA molecule, the proposed arrangement of FA molecules in the interlayer of ZLH was assembled in bilayer stacking. Such an arrangement maximizes π–π interactions between the interlayer anions, hydrogen bonding interaction between the layer OH groups and the phenolic OH groups of the anions, as well as the interaction between the layers and anions [36].

Infrared spectroscopy

The FTIR spectra of ZnO, pure FA and ZLH-FA nanocomposites are shown in Figure 5. The FTIR spectrum of pure ZnO (reagent ACS, Acros Organics) displayed a characteristic peak at 402 cm^{-1}, which is due to vibration of zinc and oxygen sub lattices [37] and is in agreement with Hussein et al. (2010). The FTIR spectrum of pure FA showed a strong characteristic vibration at 3430 cm^{-1}, which indicates O-H stretching. A

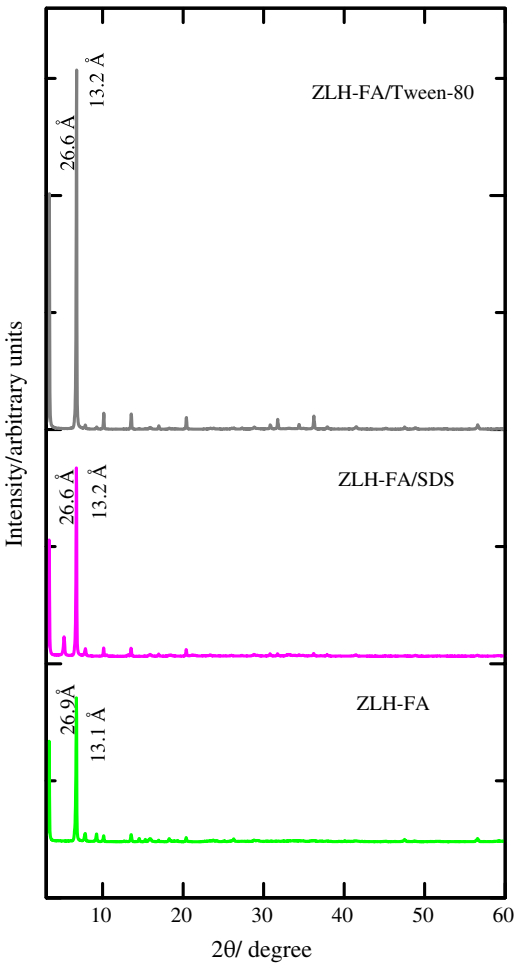

Figure 2. Powder X-ray diffraction of ZLH-FA, ZLH-FA/SDS and ZLH-FA/Tween-80 nanocomposites.

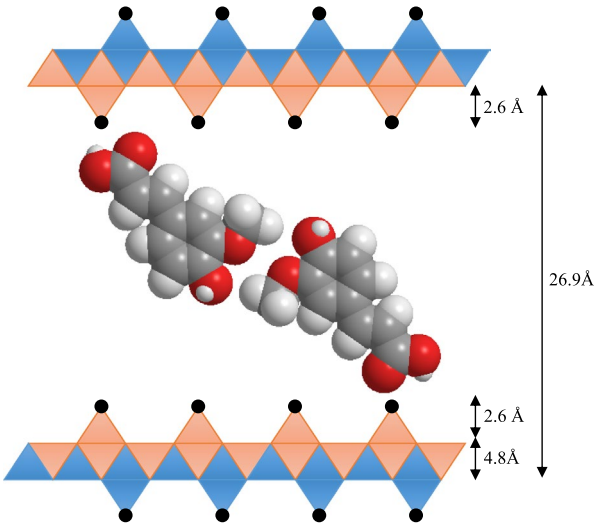

Figure 3. Proposed spatial orientation of FA in ZLH inorganic interlayer.

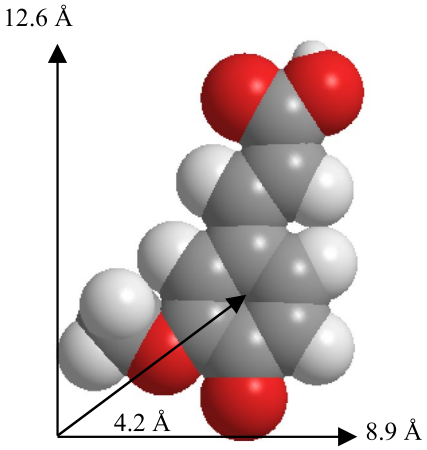

Figure 4. 3D-molecular structure of FA.

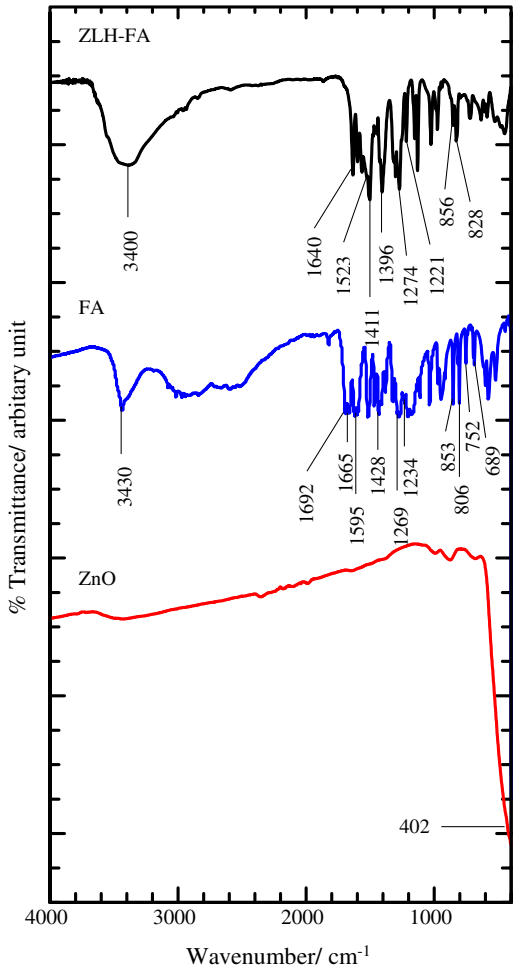

Figure 5. FTIR spectrum of ZnO, FA and ZLH-FA nanocomposite.

characteristic band of FA at 1692 cm^{-1} corresponds to stretching vibration of an undissociated carboxylic group (COOH), while those at 1595 and 1428 cm^{-1} refer to the aromatic nucleus of FA [38]. The bands at 1269 and 1234 cm^{-1} are due to ν_{as} (COC) and ν_{s} (COC).

The FTIR spectrum of ZLH-FA nanocomposite illustrates bands characteristic of pure FA, indicating successful intercalation of the FA moiety into ZLH interlayers. Some of the bands are slightly shifted in position due to interaction between ferulate anions as a host interlayer. The band attributable to a carboxylic group (COOH) disappeared because hydrogen ions in the FA molecules were removed and the FA was intercalated in anionic form. The ZLH-FA spectrum also shows the absorption bands at 1523 and 1396 cm^{-1} that were assigned to the asymmetric and symmetric carboxylate stretching modes of FA anions [36]. A band at 3400 cm^{-1} was attributed to OH stretching vibrations. The vibration bands of FA and ZLH-FA nanocomposite are listed in Table 1.

FTIR spectra of SDS and ZLH-FA/SDS nanocomposites are shown in Figure 6. The SDS displays two prominent vibrations at 2917–2849 and 1467 cm^{-1}, corresponding to the asymmetric

and symmetric CH_2 and C–H bending vibrations [39], whereas the ZLH-FA/SDS nanocomposite shows bands at 2917, 2849 and 1513 cm^{-1} for the same functional groups. An absorption band at 3480 cm^{-1} was attributed to the OH stretching in the SDS molecule. Even though the presence was surprising, it is not impossible due to the absorption of moisture during preparation of the KBr pellet [40]. The band that was correspond to the assymmetric sulphate group can be observed in both FTIR spectra of SDS and ZLH-FA/SDS at 1217 and 1219 cm^{-1}, respectively. However, the absorption bands of the asymmetric and symmetric sulphate group at 1219 and 1084 cm^{-1} in SDS cannot be observed in the ZLH-FA/SDS nanocomposite. This might due to the chemical interaction of SDS with the surface of ZLH [21].

Table 1. Fourier transforms infrared vibration bands for FA and ZLH-FA nanocomposite.

Functional groups	FA	ZLH-FA
ν (O–H)	3430 for O–H in COOH	3400 in the layer, H_2O
ν (C=O) in COOH	1692	–
ν_{as} (COO^-)	–	1523
ν_s (COO^-)	–	1396
ν (C=C); aromatic ring	1595	1640
	1428	1411
ν_{as} (C–O–C)	1269	1274
ν_s (C–O–C)	1234	1221
C–H out of plane bending	853	856
	806	828
	752	
	689	

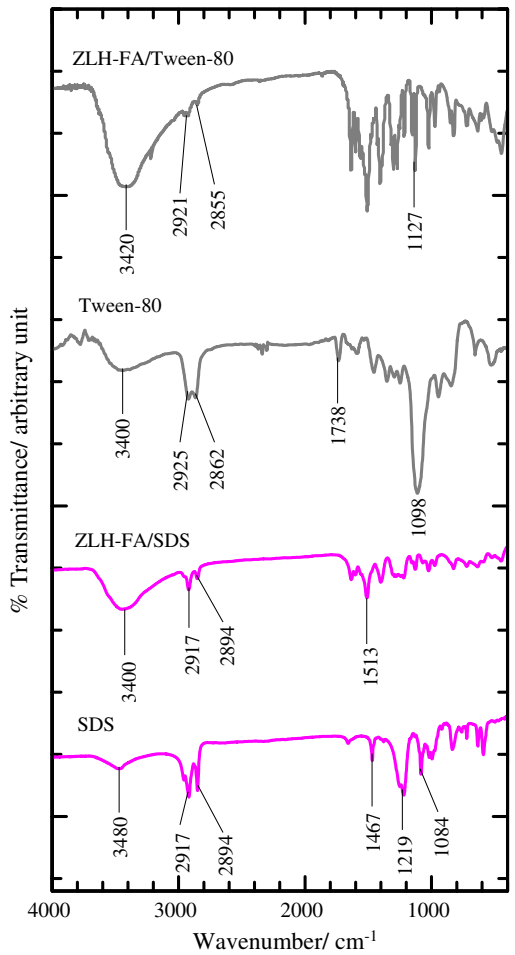

Figure 6. FTIR spectrum of SDS, ZLH-FA/SDS nanocomposite, Tween-80 and ZLH-FA/Tween-80 nanocomposite.

The FTIR spectrum of Tween-80 shows an absorption band at 2925 cm^{-1} which belongs to a methyl group (-CH_3) while the band at 2862 cm^{-1} is due to -CH_2 stretching The absorption bands at 1738 , 1098 and 3400 cm^{-1}were due to stretching vibrations of C=O, C-O-C and OH groups, respectively. The FTIR spectrum of ZLH-FA/Tween-80 nanocomposite shows the characteristic peaks of CH_2 at 2855 cm^{-1}, CH_3 at 2921 cm^{-1}, C-O-C at 1127 cm^{-1} and a broad band due to OH groups at 3420 cm^{-1}. The presence of most of the peaks of Tween-80 in the FTIR spectrum of ZLH-FA/Tween-80 nanocomposite supports the presence of Tween-80 on its surface. However, the absorption band of C=O stretching was not observed in the spectrum of ZLH-FA/Tween-80 nanocomposite due to the chemical interaction of Tween-80 with the surface of ZLH via the oxygen of C=O group [41]. The chemical structure of FA, SDS and Tween-80 were shown in Figure 7.

Elemental analysis

Elemental analysis of the ZnO and ZLH-FA nanocomposite are shown in Table 2. Elemental analysis showed a high percentage of Zn for the pure commercial ZnO used in this work, with a value of 81·46%. CHNS analysis showed that the ZLH-FA contained 35·14% carbon (w/w), 3·55% hydrogen (w/w), and no nitrogen in the material. Elemental analysis showed 43·70% zinc (w/w). The loading percentage of the FA drug in the ZLH-FA nanocomposite was 56·82% (w/w). As expected, the ZLH-FA nanocomposite contained both organic and inorganic constituents, and thus supported the successful intercalation of the FA drug into the interlayer galleries of ZLH. From the elemental analysis and thermogravimetric

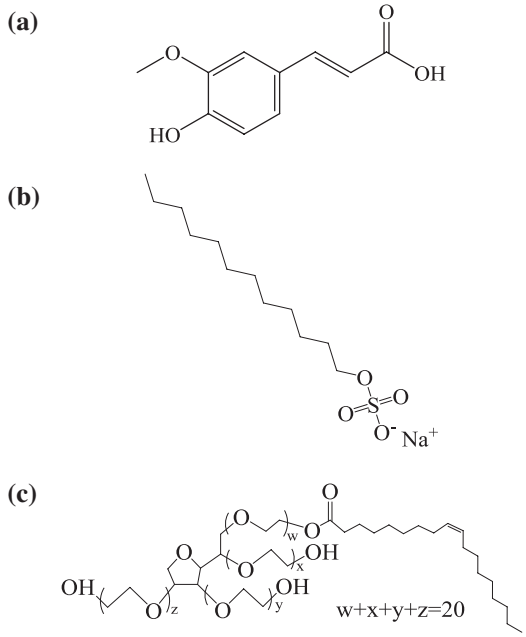

Figure 7. Chemical structure of (a) ferulic acid, (b) sodium dodecylsulphate and (c) Tween-80.

Table 2. The analysed chemical compositions of ZnO and the ZLH-FA nanocomposites.

Sample	C (%)	H (%)	N (%)	Zn (% w/w)	[a]FA (% w/w)
ZnO	–	–	–	81·47	–
ZLH-FA	35·14	3·55	–	43·67	56·82

[a]Estimated using CHNS analysis.

studies, the formula for the nanocomposite can be proposed as $Zn(OH)_{1.29}(OHCH_3OC_6H_3CHCHCOO^-)_{0.71}.0.91H_2O$.

Thermal analysis

TGA and DTG profiles of the ZnO, FA, ZLH-FA nanocomposite, SDS, ZLH-FA/SDS nanocomposite, Tween-80 and ZLH-FA/Tween-80 nanocomposite are shown in Figure 8 and weight loss data is summarised in Table 3.

As shown in Figure 8(a), the TGA/DTG thermograms of pure FA showed a single sharp weight loss of 100% at a maximum temperature of 255 °C, which can be attributed to complete combustion of FA. After the intercalation process, the thermal behaviour of the resulting product was significantly different from that of the precursor. The thermal decomposition of ZLH-FA nanocomposite (Figure 8(b)) showed three stages of weight loss, which occurred at maximum temperatures of 77, 335 and 468 °C with weight losses of 6·7, 16·6 and

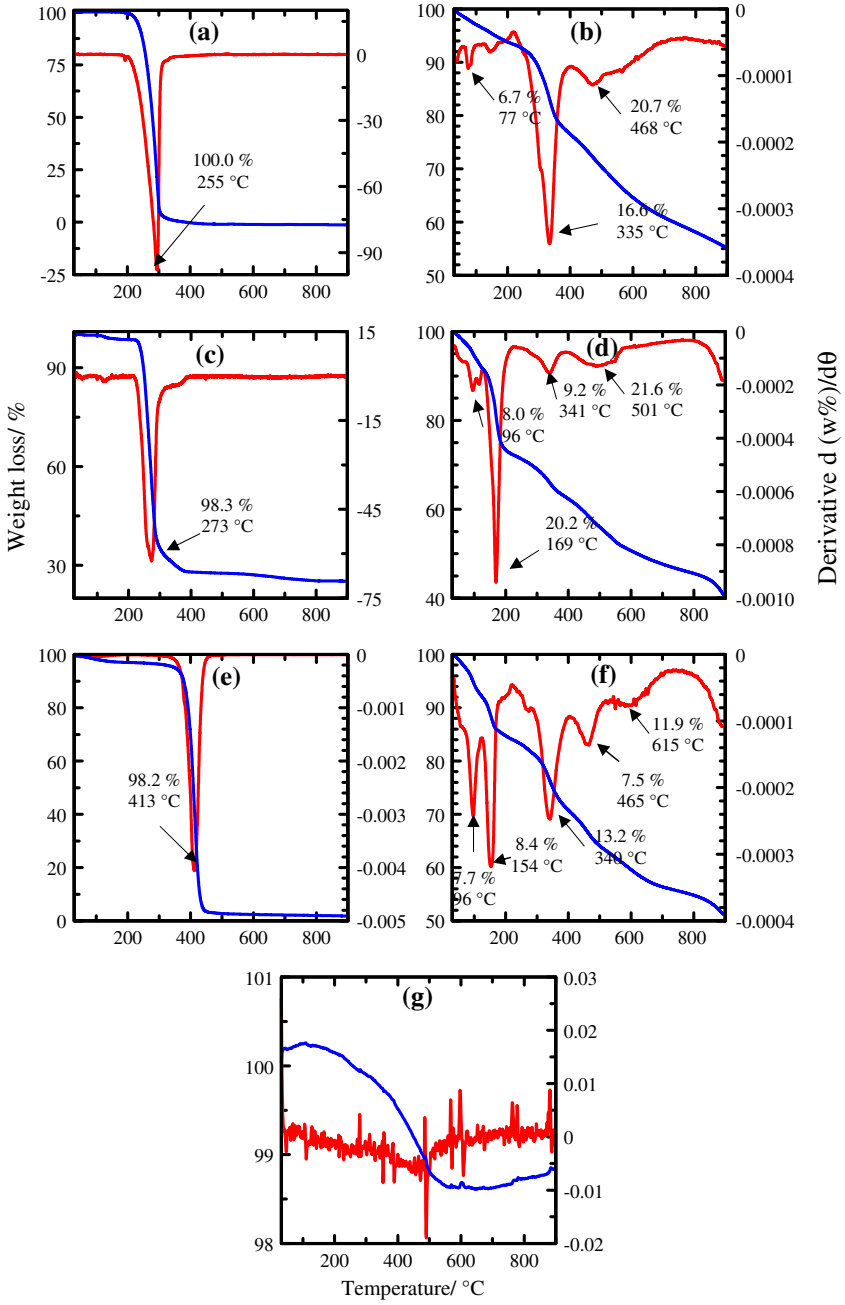

Figure 8. TGA/DTG thermograms of (a) FA, (b) ZLH-FA nanocomposite, (c) SDS, (d) ZLH-FA/SDS nanocomposite, (e) Tween-80, (f) ZLH-FA/Tween-80 nanocomposite and (g) ZnO.

Table 3. TGA/DTG data of weight loss for FA, ZLH-FA, SDS, ZLH-FA/SDS and ZLH-FA/Tween-80 nanocomposites.

	Weight loss			
Temperature(°C)	35–200	201–600	601–1000	Total weight loss (%)
FA	100·0 (T_{max} = 255 °C)	–	–	100·0
ZLH-FA	6·7 (T_{max} = 77 °C)	37·3 (T_{max} = 468 °C)	–	44·0
SDS		98·3 (T_{max} = 273 °C)		98·3
ZLH-FA/SDS	28·2 (T_{max} = 169 °C)	30·8 (T_{max} = 501 °C)	–	59·0
ZLH-FA/Tween-80	16·1 (T_{max} = 154 °C)	20·7 (T_{max} = 465 °C)	11·9 (T_{max} = 615 °C)	48·7

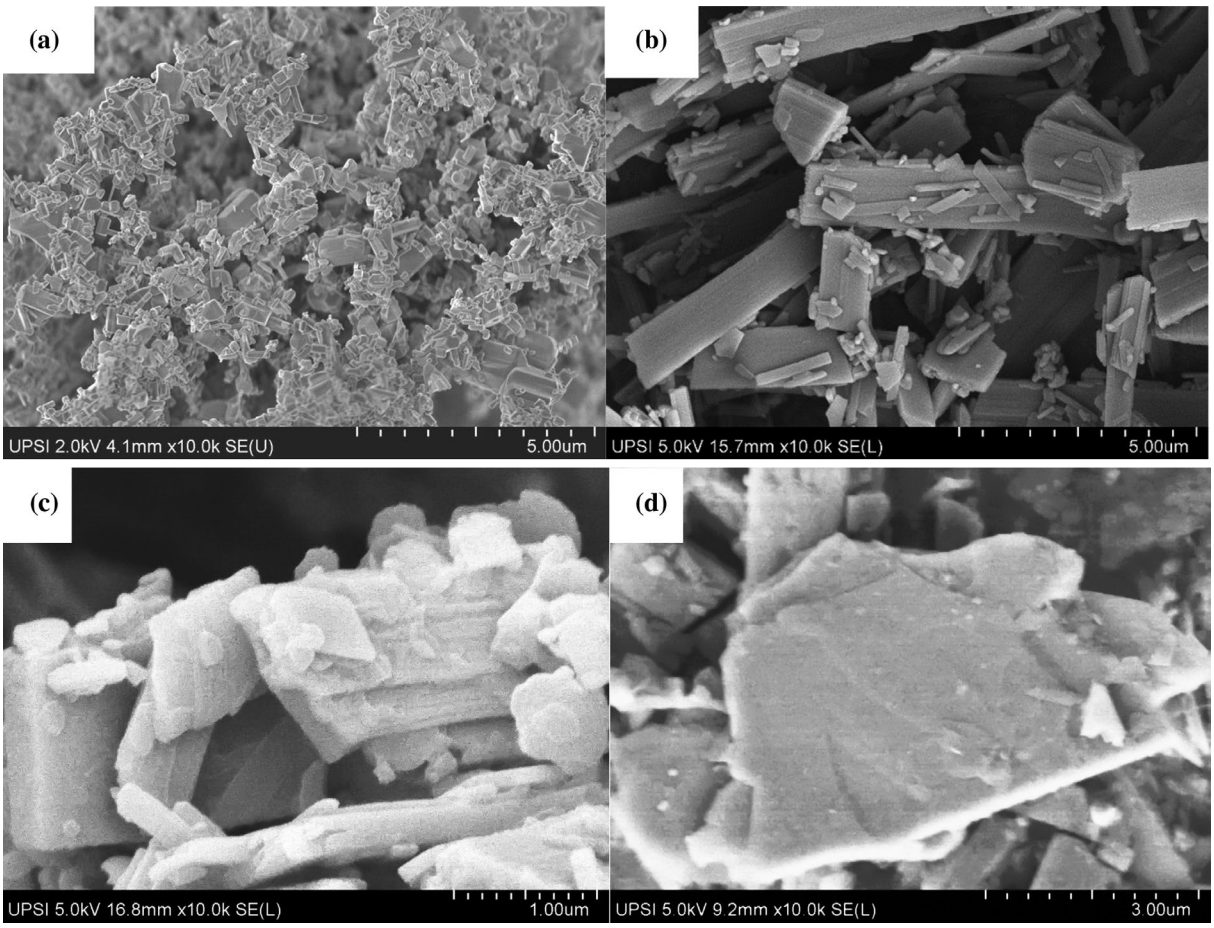

Figure 9. FESEM images of (a) ZnO, (b) ZLH-FA, (c) ZLH-FA/SDS and (d) ZLH-FA/Tween-80 nanocomposites at 10 K magnification.

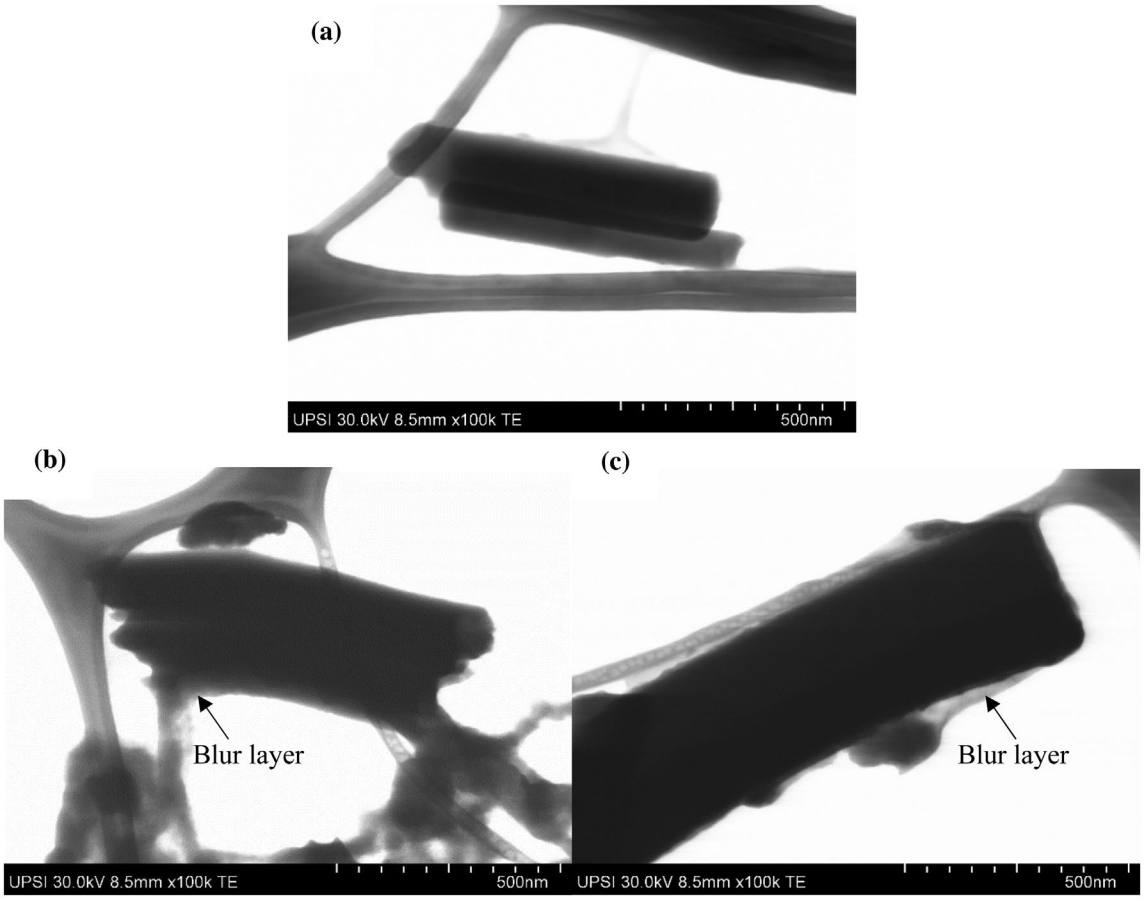

Figure 10. TEM images of (a) ZLH-FA nanocomposite and (b) ZLH-FA/SDS and (c) ZLH-FA/Tween-80 nanocomposite at 100 K magnification.

20·7% respectively. The first stage in the region of 55–119 °C can be associated with the removal of the surface-physisorbed water molecules. The second stage of weight loss corresponds to the dehydroxylation of the hydroxide layers, as well as partial decomposition of the intercalated FA anions [20]. The third stage recorded a 20·7% weight loss with the major peak around 550 °C, and was due to the complete decomposition of intercalated FA anions [42]. As shown in Figure 8(g), TGA curve shows about 1% of weight loss of ZnO with no maximum temperature indicates that pure ZnO is a thermally stable compound. A higher temperature is required for total degradation of ZnO thus make it perfect candidate as a starting material in synthesising ZLH-FA nanocomposite [43,44]. It can be seen that the maximum temperature region of ZLH-FA nanocomposite is obviously higher than free pure FA, suggesting that the inorganic layers of ZLH enhanced the thermal stability of FA, the organic moiety.

The thermal decomposition of SDS, Tween-80, ZLH-FA/SDS nanocomposite, Tween-80 and ZLH-FA/Tween-80 nanocomposite are shown in Figure 8(c)–(f), respectively. In Figure 8(c), the SDS shows only a single stage of weight loss at a maximum temperature of 273 °C, attributed to the complete combustion of SDS. The ZLH-FA/SDS nanocomposite (Figure 8(d)) exhibits a more complicated thermal behaviour than ZLH-FA nanocomposite. The coated nanocomposite, ZLH-FA/SDS, showed four major stages of weight loss. These occurred at maximum temperatures of 96, 169, 341 and 501 °C with weight loss of 8·0, 20·2, 9·2 and 21·6%, respectively. The first stage of weight loss in the range 72–131 °C was attributed to the removal of surface and water in the interlayer. The second weight loss stage was due to the loss of SDS on the surface of ZLH-FA/SDS nanocomposite, which usually overlapped with loss of an alkyl group at a temperature range from 131 to 224 °C [45]. The third and fourth stages of weight losses, in the region from 224 to 594 °C, were attributed to the fully dehydroxylation and elimination of intercalated FA anions.

In Figure 8(e), TGA of Tween-80 showed a strong, intense and sharp peak at a maximum temperature of 413 °C, with weight loss of 98·2%. This corresponded to complete combustion decomposition of Tween-80. In contrast with ZLH-FA nanocomposite, the coated nanocomposite ZLH-FA/Tween-80 exhibited a more complicated thermal behaviour, with four stages of weight loss. The first stage spanned the 30–123 °C region, with a 7·7% weight loss, which was due to the removal of the surface-physisorbed water molecules. The second stage in the range 123–225 °C accounted for a weight loss of 8·4%, and was attributed to the removal of water molecules from the intercalated structure, as well as decomposition of surfactant [46,47]. The third weight loss stage was due to dehydroxylation of the hydroxide layers, with a percentage of 13·2%, which could be seen at 225–400 °C. The fourth stage spanned the range 400–700 °C, with a 19·4% weight loss corresponding to the thermal decomposition of organic species and ferulate anions, leaving only a relatively less volatile, metal oxide [48].

As shown in Table 3, the total weight losses of ZLH-FA/SDS and ZLH-FA/Tween-80 nanocomposites were much higher

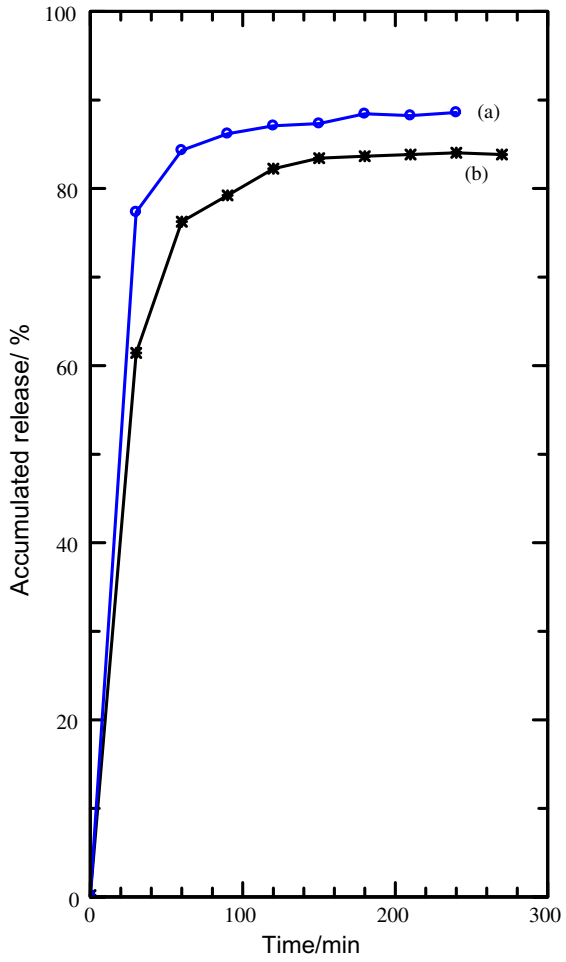

Figure 11. Release profile of FA from ZLH-FA into phosphate buffer solution at pH (a) 4.8 and (b) 7.4.

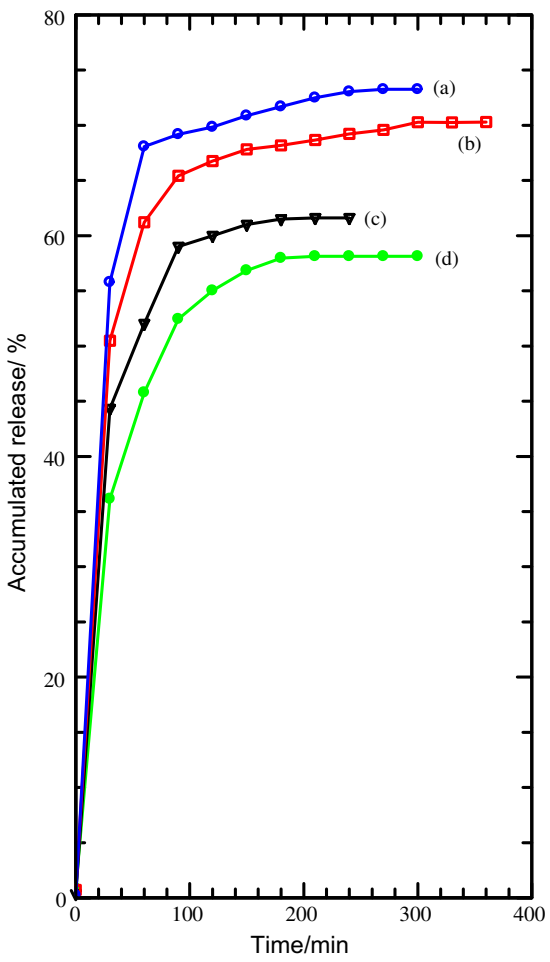

Figure 12. Release profile of FA from ZLH-FA/SDS into phosphate buffer solution at pH (a) 4.8 and (b) 7.4, and from ZLH-FA/Tween-80 at pH (c) 4.8 and (b) 7.4.

than ZLH-FA nanocomposite. By comparing these weight losses, it can be concluded that the ZLH-FA nanocomposite was coated with 15% SDS and 4·7% Tween-80 [21]. The temperature region after coating was markedly enhanced, clearly showing that the degradation behaviour of both coated materials improved.

Morphology analysis

The morphology of ZnO, ZLH-FA, ZLH-FA/SDS and ZLH-FA/Tween-80 nanocomposites is shown in Figure 9. The ZnO morphology (Figure 9(a)) reveals a non-uniform granular structure without any specific shape and size [4]. As shown in Figure 9(b), the non-uniform structure was transformed into a plate-like structure with irregular size and shape, as the intercalation of ferulate anions into the interlayer galleries of ZLH took place. A slight morphological change could be observed after the coating process using SDS and Tween-80 surfactants. The plate-like structure of ZLH-FA/SDS (Figure 9(c)) and ZLH-FA/Tween-80 (Figure 9(d)) nanocomposites were surrounded by small agglomeration, with smooth surface which clearly differentiated between coated and uncoated materials.

Transmission electron microscopy analysis

The TEM images of ZLH-FA, ZLH-FA/SDS and ZLH-FA/Tween-80 nanocomposites are shown in Figure 10(a)–(c), respectively. The morphology of the coated and uncoated nanocomposites was slightly different from each other. After coating by SDS and Tween-80 surfactants, a grey and blurred contrast layer around the ZLH-FA/SDS nanocomposite and ZLH-FA/Tween-80 nanocomposite was observed. The resulting morphology was considered as SDS and Tween-80 coated on the surface of ZLH-FA nanocomposites similarly as reported by Li et al. [49] and Tang et al. [50].

Controlled release study of FA from interlayers of ZLH-FA, ZLH-FA/SDS and ZLH-FA/Tween-80 nanocomposites

The release profiles of FA from the interlayer of the ZLH-FA nanocomposite (Figure 11) were done in phosphate buffer solution at pH 4·8 and 7·4. As mentioned before, a phosphate buffer solution with different pH values was used to examine whether the release of FA was affected by pH or not. As shown in Figure 11, the release rate of the FA from the interlayer of the ZLH-FA nanocomposite at pH 7·4 was

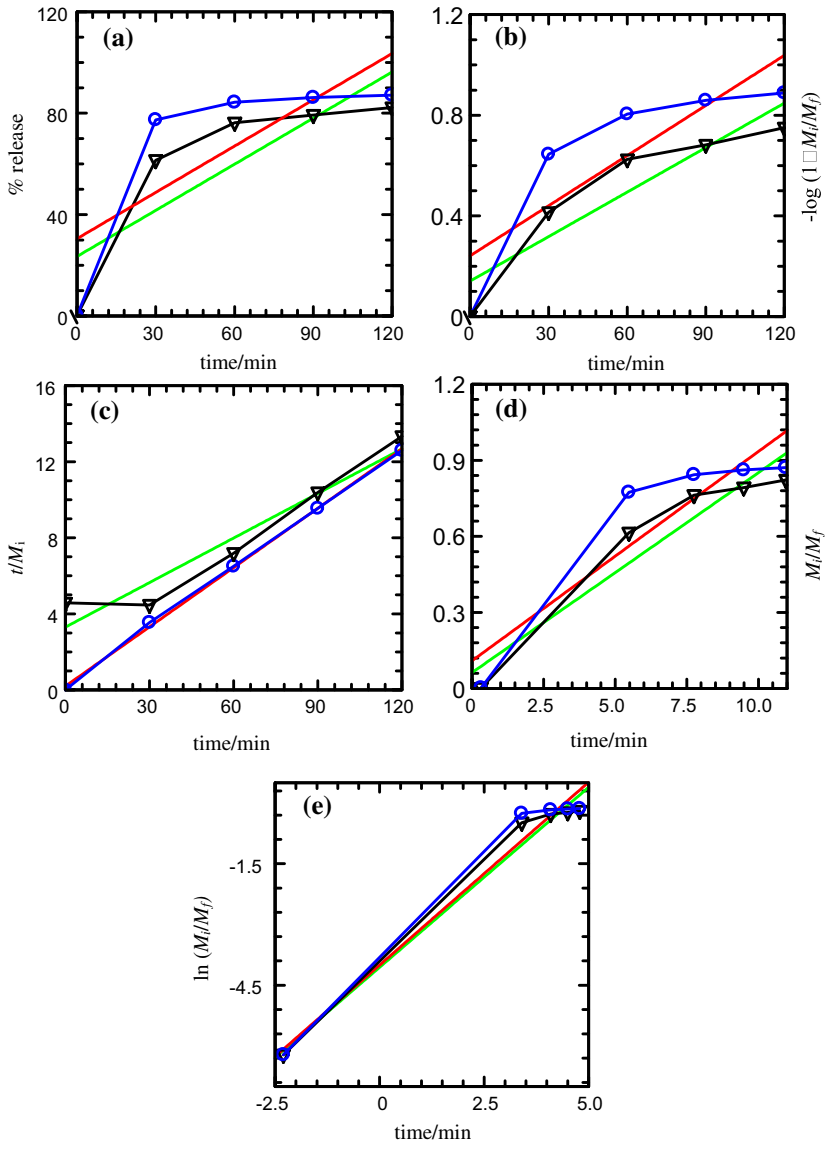

Figure 13. Fitting of the data of FA released from ZLH-FA nanocomposite into phosphate buffer solution at pH 4.8 (blue) and 7.4 (black) to the (a) zeroth, (b) first, (c) pseudo second order, (d) parabolic diffusion and (e) Fickian diffusion models.

lower than that at pH 4·8, indicating that the release rate of FA from the interlayer of nanocomposites was pH-dependent. The difference in the release rates at pH 4·8 and 7·4 may be due to the difference in the release mechanism of FA from the interlayer of nanocomposites [51]. Release of FA from the interlayer of ZLH-FA nanocomposite at pH 4·8 (Figure 11(a)) showed a fast release for the first 30 min with 77%, which could possibly be attributed to partial dissolution of ZLH in acidic media. It was followed by a slower step, which was related to the ion exchange process between FA anions and the phosphate anions in the buffer solution. At equilibrium, the percentage release of FA reached approximately 89% within 240 min. As shown in Figure 11(b), the release of FA from the interlayer of ZLH-FA nanocomposite at pH 7·4 was rapid for the first 30 min with percentage release of approximately 61%, which could be attributed to the release of FA anions adsorbed on the outer surface of ZLH, as well as intercalated FA [6]. However, the release of FA from the interlayer of ZLH-FA nanocomposite at pH 7·4 was slower and more sustained, compared with the solution at pH 4·8 with total release of 84% in 270 min. The mechanism might have occurred through an ion-exchange reaction.

Figure 12 shows the release profile of FA from coated nanocomposites, ZLH-FA/SDS and ZLH-FA/Tween-80, performed using the same media, a phosphate buffer solution at pH 4·8 and 7·4. At pH 4·8 and 7·4, both coated nanocomposites showed slower release rate of FA compared to the release rate of FA from the uncoated nanocomposite. The percentage release of FA from the interlayer of the ZLH-FA/SDS nanocomposite at pH 4·8 (Figure 12(a)) and pH 7·4 (Figure 12(b)) was 73 and 70% within 300 and 360 min, respectively. Meanwhile, FA release from the interlayer of ZLH-FA/Tween-80 reached approximately 62% within 300 min at pH 4·8 (Figure 12(c)) and 58% within 330 min at pH 7·4 (Figure 12(d)). Since the duration for the releasing of FA from the coated nanocomposite is longer than uncoated nanocomposite, it showed that the modification on the external surface of the ZLH successfully enhanced the release properties of ZLH as the host. The slower release rates were attributed to the retarding effect caused by the coating of ZLH-FA nanocomposite [25]. Based on this observation, the coated ZLH-FA nanocomposite has a good potential as a controlled-release system for the FA drug anion.

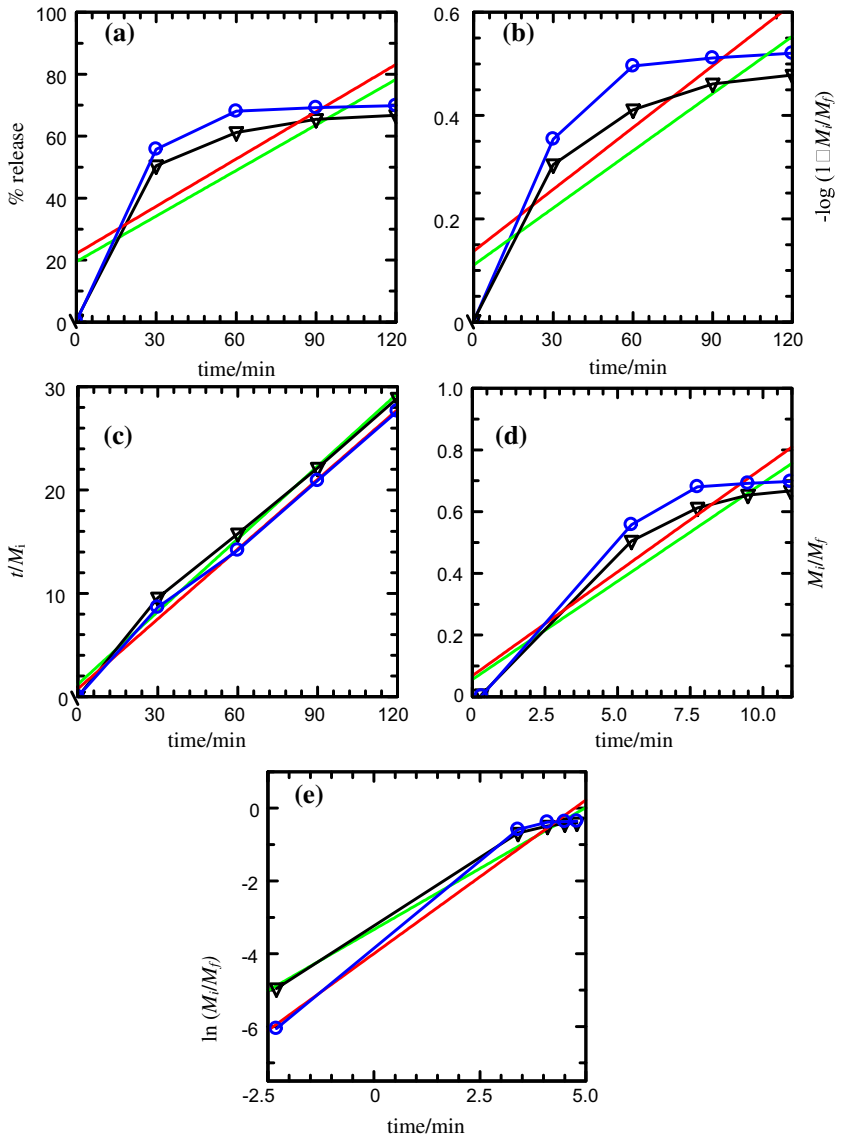

Figure 14. Fitting of the data of FA released from ZLH-FA/SDS nanocomposite into phosphate buffer solution at pH 4.8 (blue) and 7.4 (black)to the (a) zeroth, (b) first, (c) pseudo second order, (d) parabolic diffusion and (e) Fickian diffusion models.

Release kinetics of FA from interlayer of ZLH-FA, ZLH-FA/SDS and ZLH-FA/Tween-80 nanocomposites

In order to obtain the release behaviour of FA from the interlayers of the ZLH-FA nanocomposites and their coated nanocomposites, five types of kinetic models were used to fit the release data. The models used were zeroth order (Equation 4) [4], first order (Equation 5) [52], pseudo-second order (Equation 6) [53], parabolic diffusion (Equation 7) [54] and Fickian diffusion (Equation 8) [55]. The x value represents the percentage release of FA anions at time t, while M_i and M_f are the initial and final concentration of FA anions, respectively. n is an empirical parameter describing the release mechanism and c is a constant. The parameter correlation coefficients, r^2, rate constant, k and $t_{1/2}$ values were calculated from the corresponding equations.

$$x = t + c \ (1) \tag{5}$$

$$-\log\left(1-M_i/M_f\right) = t + c \ (2) \tag{6}$$

$$t/M_i = 1/M_f^2 + t/M_f \ (3) \tag{7}$$

$$M_i/M_f = kt^{0.5} + c \ (4) \tag{8}$$

$$M_i/M_f = kt^n \ (5) \tag{9}$$

The fitting data of the FA release profiles from the interlayers of ZLH-FA, ZLH-FA/SDS and ZLH-FA/Tween-80 nanocomposites based on the five kinetic models are shown in Figures 13–15, respectively. The correlation coefficients (r^2) are tabulated in Table 4. As shown in Table 4, it can be seen that the release of FA from the interlayer of the ZLH-FA nanocomposite followed the pseudo-second order model very well for both pH values, with satisfactory coefficients of 0·999 (pH 4·8) and 0·930 (pH 7·4). It was found that the pseudo-second order kinetic model also provided a better fit than the other models for release of FA from the coated nanocomposites, ZLH-FA/SDS and ZLH-FA/

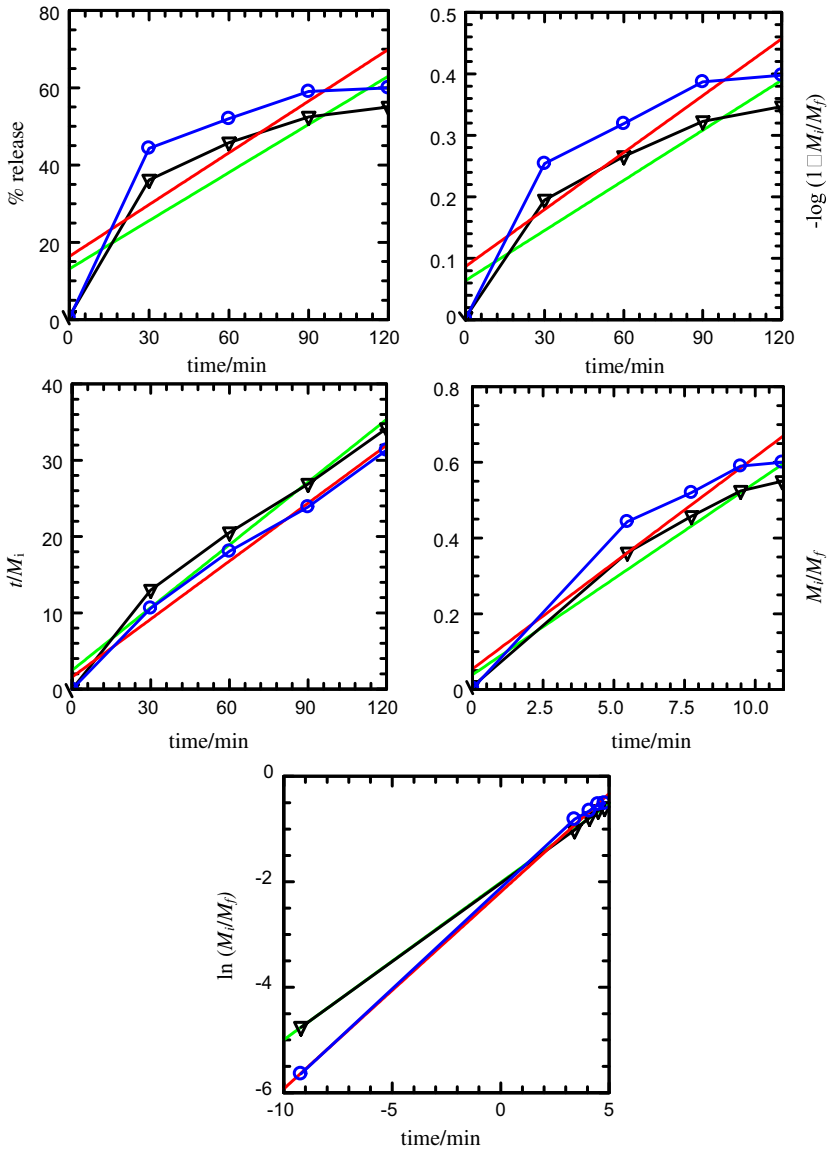

Figure 15. Fitting of the data of FA released from ZLH-FA/Tween-80nanocomposite into phosphate buffer solution at pH 4.8 (blue) and 7.4 (black)to the (a) zeroth, (b) first, (c) pseudo second order, (d) parabolic diffusion and (e) Fickian diffusion models.

Table 4. Correlation coefficient (r^2), rate constant (k), and half-life ($t_{1/2}$) values obtained by fitting the data of the release of FA from ZLH-FA, ZLH-FA/SDS and ZLH-FA/Tween-80 nanocomposites into phosphate buffer solution at (a) pH 4·8 and (b) pH 7·4.

		Zeroth order	First order	Parabolic diffusion	Fickian diffusion	Pseudo-second order			
Samples	pH	r^2				r^2	k ($\times 10^{-2}$) s^{-1}	$t_{1/2}$ (min)	c
ZLH-FA	4·8	0·591	0·726	0·835	0·974	0·999	4·79	2·17	0·20
ZLH-FA	7·4	0·703	0·849	0·913	0·982	0·930	0·48	16·26	3·30
ZLH-FA/SDS	4·8	0·653	0·735	0·881	0·979	0·996	4·48	5·02	1·13
ZLH-FA/SDS	7·4	0·705	0·799	0·915	0·985	0·993	4·15	5·66	1·33
ZLH-FA/Tween-80	4·8	0·734	0·818	0·737	0·989	0·988	4·03	6.28	1·59
ZLH-FA/Tween-80	7·4	0·800	0·873	0·782	0·994	0·978	3·04	9·01	2·47

Tween-80. The r^2 values for the ZLH-FA/SDS nanocomposite were 0·996 and 0·993 for pH 4·8 and 7·4, respectively, whereas they were 0·988 (pH 4·8) and 0·978 (pH 7·4) for the ZLH-FA/Tween-80 nanocomposite. The pseudo-second order model described the release process of FA anions from the inorganic ZLH involved in the dissolution of nanocomposites, as well as the ion exchange between the intercalated anions in the interlayer of ZLH and the phosphate anions in the aqueous solution [55]. There is quite a big gap for the k, t½ and c values for the release of ZLH-FA in solution at pH 7·4 and pH 4·8. At an acidic pH (pH 4·8), ZLH may be easily dissolved and the release of the interlayer anions might occur due to the disintegration of the ZLH interlayers together with the ion exchange process [56]. On the contrary, at pH 7·4, ZLH are more stable, and as a result, release would occur through an anion exchange process involving the intergallery of ZLH. This result is similar to the kinetic study for the release of protocatechuate done by Barahuie et al. [18].

Conclusion

In the present work, the ferulate drug anion was successfully intercalated into ZLH interlayers using a direct reaction method using ZnO as a precursor to obtain a new nanocomposite, namely ZLH-FA with a basal spacing of 26·9 Å. XRD analysis proved that SDS and Tween-80 were formed on the surface of ZLH particles, without an exchange with intercalated ferulate anions, thus forming a ZLH-FA/SDS and ZLH-FA/Tween-80 nanocomposite. The release study showed that the release of FA from the ZLH-FA nanocomposite into a phosphate buffer solution was slow and sustained, with a total equilibrium of 89% and 84% when exposed to pH 4·8 and 7·4, respectively. However, the release of FA became slow after ZLH-FA nanocomposite was coated with SDS and Tween-80 due to a retarding effect. A kinetic study showed that both uncoated and coated nanocomposites were governed by a pseudo-second order kinetic model for both pH 4·8 and 7·4. Hence, the present results demonstrate that ZLH materials have great potential to be used as a host for controlled release formulations of FA anions. Hence, the present results demonstrate that coated ZLH materials have great potential to be used as a formulation for controlled release system of FA anions.

Contributors

NH Conceived and designed the study, obtained funded and ethics approval, wrote the article in whole/part, revised the article. SNMS Collected and analysed the data, wrote the article in whole/part, revised the article. ZM Collected and analysed the data, wrote the article in whole/part, revised the article. IMI Analysed the data, wrote the article in whole/part, revised the article, obtained funded and ethics approval. NMA Collected and analysed the data, revised the article. SAB Collected and analysed the data, revised the article. SMS Analysed the data, revised the article. MZH Analysed the data, revised the article.

Disclosure statement

No potential conflict of interest was reported by the authors.

Funding

The author wishes to thank UPSI and Ministry of Education for support during this research. This work was supported under GPU [grant number 2017–0188-101-01] and FRGS [grant number 2017–0075–101–02].

References

[1] Arizaga GGC, Satyanarayana KG, Wypych F. Layered hydroxide salts: synthesis, properties and potential applications. Solid State Ionics. 2007;178:1143–1162.
[2] Hussein MZ, Rahman NSSA, Sarijo SH, et al. Herbicide-intercalated zinc layered hydroxide nanohybrid for a dual-guest controlled release formulation. Int J Mol Sci. 2012;13:7328–7342.
[3] Hussein MZ, Nazarudin NFB, Sarijo SH, et al. Synthesis of a layered organic-inorganic nanohybrid of 4- chlorophenoxyacetate-zinc-layered hydroxide with sustained release properties. J Nanomater. 2012;2012:1–10.
[4] Hussein SamerMZ, Al Ali SH, Zainal Z, et al. Development of antiproliferative nanohybrid compound with controlled release property using ellagic acid as the active agent. Int J Nanomed. 2011;6:1373–1383.
[5] Al Ali SHH, Al-Qubaisi M, Hussein SamerMZ, et al. Preparation of hippurate-zinc layered hydroxide nanohybrid and its synergistic effect with tamoxifen on HepG2 cell lines. Int J Nanomed. 2011;6:3099–3111.
[6] Al Ali SHH, Al-Qubaisi M, Hussein MZ, et al. Controlled release and angiotensin-converting enzyme inhibition properties of an antihypertensive drug based on a perindopril erbumine-layered double hydroxide nanocomposite. Int J Nanomed. 2012;7:2129–2141.
[7] Kandare E, Chigwada G, Wang D, et al. Probing synergism, antagonism, and additive effects in poly(vinyl ester) (PVE) composites with fire retardants. Polym Degrad Stab. 2006;91:1209–1218.
[8] Rocca E, Caillet C, Mesbah A, et al. Intercalation in zinc-layered hydroxide: zinc hydroxyheptanoate used as protective material on zinc. Chem Mater. 2006;18:6186–6193.
[9] Trikeriotis M, Ghanotakis DF. Intercalation of hydrophilic and hydrophobic antibiotics in layered double hydroxides. Int J Pharm. 2007;332:176–184.
[10] Barahuie F, Hussein MZ, Fakurazi S, et al. Development of drug delivery systems based on layered hydroxides for nanomedicine. Int J Mol Sci. 2014;15:7750–7786.
[11] Manzano M, Aina V, Areán CO, et al. Studies on MCM-41 mesoporous silica for drug delivery: effect of particle morphology and amine functionalization. Chem Eng J. 2008;137:30–37.
[12] Giri TK, Kumar K, Alexander A, et al. A novel and alternative approach to controlled release drug delivery system based on solid dispersion technique. Bull Fac Pharmacy Cairo Univ. 2012;50:147–159.
[13] Xu ZP, Zeng QH, Lu GQ, et al. Inorganic nanoparticles as carriers for efficient cellular delivery. Chem Eng Sci. 2006;61:1027–1040.

[14] Wu X, Tan Y, Mao H, et al. Toxic effects of iron oxide nanoparticles on human umbilical vein endothelial cells. Int J Nanomed. 2010;5:385–399.
[15] Shi W, Wei M, Jin L, et al. Calcined layered double hydroxides as a "biomolecular vessel" for bromelain: Immobilization, storage and release. J Mol Catal B Enzym. 2007;47:58–65.
[16] Hasan S, Al Ali H, Al-qubaisi M, et al. Controlled-release formulation of antihistamine based on cetirizine zinc-layered hydroxide nanocomposites and its effect on histamine release from basophilic leukemia (RBL-2H3) cells. Int J Nanomed. 2012;7:3351–3363.
[17] Mohsin SMN, Hussein MZ, Sarijo SH, et al. Synthesis of (cinnamate-zinc layered hydroxide) intercalation compound for sunscreen application. Chem Cent J. 2013;7:26–38.
[18] Barahuie F, Hussein MZ, Abd Gani S, et al. Anticancer nanodelivery system with controlled release property based on protocatechuate-zinc layered hydroxide nanohybrid. Int J Nanomed. 2014;9:3137–3149.
[19] Saifullah B, Arulselvan P, El Zowalaty ME, et al. Development of a highly biocompatible antituberculosis nanodelivery formulation based on para-aminosalicylic acid – zinc layered hydroxide nanocomposites. Sci World J. 2014;2014:1–12.
[20] Latip AFA, Hussein MZ, Stanslas J, et al. Release behavior and toxicity profiles towards A549 cell lines of ciprofloxacin from its layered zinc hydroxide intercalation compound. Chem Cent J. 2013;7:119–130.
[21] Kura AU, Hussein-Al-Ali SH, Hussein MZ, et al. Preparation of tween 80-Zn/Al-levodopa-layered double hydroxides nanocomposite for drug delivery system. Sci World J. 2014;2014:1–10.
[22] Das D, Lin S. viaDouble-coated poly (butylcynanoacrylate) nanoparticulate delivery systems for brain targeting of dalargtin via oral administration. J Pharm Sci. 2005;94:1343–1353.
[23] Dong L, Gou G, Jiao L. Characterization of a dextran–coated layered double hydroxide acetylsalicylic acid delivery system and its pharmacokinetics in rabbit. Acta Pharm Sin B. 2013;3:400–407.
[24] Kim T-HT-H, Lee J-AJ-A, Choi S-JS-J, et al. Polymer coated CaAl-Layered double hydroxide nanomaterials for potential calcium supplement. Int J Mol Sci. 2014;15:22563–22579.
[25] Kameshima Y, Sasaki H, Isobe T, et al. Synthesis of composites of sodium oleate/Mg-Al-ascorbic acid-layered double hydroxides for drug delivery applications. Int J Pharm. 2009;381:34–39.
[26] Wei PR, Cheng SH, Liao WN, et al. Synthesis of chitosan-coated near-infrared layered double hydroxide nanoparticles for *in vivo* optical imaging. J Mater Chem. 2012;22:5503.
[27] Ou S, Kwok KC. Ferulic acid: pharmaceutical functions, preparation and applications in foods. J Sci Food Agric. 2004;84:1261–1269.
[28] Ergün BÇ, Çoban T, Onurdag FK, et al. Synthesis, antioxidant and antimicrobial evaluation of simple aromatic esters of ferulic acid. Arch Pharm Res. 2011;34:1251–1261.
[29] Saifullah B, Hussein MZ, Hussein-Al-Ali SH, et al. Sustained release formulation of an anti-tuberculosis drug based on para-amino salicylic acid-zinc layered hydroxide nanocomposite. Chem Cent J. 2013;7:72–83.
[30] Bashi AM, Hussein MZ, Zainal Z, et al. Synthesis and controlled release properties of 2,4-dichlorophenoxy acetate-zinc layered hydroxide nanohybrid. J Solid State Chem. 2013;203:19–24.
[31] Arizaga GGC, Gardolinski JEFDC, Schreiner WH, et al. Intercalation of an oxalatooxoniobate complex into layered double hydroxide and layered zinc hydroxide nitrate. J Colloid Interface Sci. 2009;330:352–358.
[32] Hussein MZ, Hashim N, Yahaya AH, et al. Synthesis and characterization of [4-(2,4-dichlorophenoxybutyrate)-zinc layered hydroxide] nanohybrid. Solid State Sci. 2010;12:770–775.
[33] Xingfu Z, Zhaolin H, Yiqun F, et al. Microspheric organization of multilayered ZnO nanosheets with hierarchically porous structures. J Phys Chem C. 2008;112:11722–11728.
[34] Bang S, Lee S, Ko Y, et al. Photocurrent detection of chemically tuned hierarchical ZnO nanostructures grown on seed layers formed by atomic layer deposition. Nanoscale Res Lett. 2012;7:290–300.
[35] Stählin W, Oswald HR. The crystal structure of zinc hydroxide nitrate, Zn5(OH)8(NO3)2.2H2O. *Acta Crystallogr Sect B Struct Crystallogr Cryst Chem*. 1970;26:860–863.
[36] Biswick T. Park D-HH, Choy J-HH. Enhancing the UV A1 screening ability of caffeic acid by encapsulation in layered basic zinc hydroxide matrix. J Phys Chem Solids. 2012;73:1510–1513.
[37] Muñoz-Espí R, Chandra A, Wegner G. Crystal perfection in zinc oxide with occluded carboxyl-functionalized latex particles. Cryst Growth Des. 2007;7:1584–1589.
[38] Kim H, Ryu K, Kang J, et al. Anticancer activity of ferulic acid-inorganic nanohybrids synthesized via two different hybridization routes, reconstruction and exfoliation-reassembly. Sci World J. 2013;2013:1–9.
[39] Viana RB, daSilva ABF, Pimentel AS. Infrared spectroscopy of anionic, cationic, and zwitterionic surfactants. Adv Phys Chem. 2012;2012.
[40] Hussein MZB, Zainal Z, Ming CY. Microwave-assisted synthesis of Zn-Al-layered double hydroxide-sodium dodecyl sulfate nanocomposite. J Mater Sci Lett. 2000;19:879–883.
[41] Khan Y, Durrani SK, Siddique M, et al. Hydrothermal synthesis of alpha Fe2O3 nanoparticles capped by Tween-80. Mater Lett. 2011;65:2224–2227.
[42] Schouten N, van der Ham LGJ, Euverink G-JW, et al. Optimization of layered double hydroxide stability and adsorption capacity for anionic surfactants. Adsorption. 2007;13:523–532.
[43] Weidenkaff A, Reller AW, Wokaun A, et al. Thermogravimetric analysis of the ZnO/Zn water splitting cycle. Thermochim Acta. 2000;359:69–75.
[44] Liufu SC, Xiao HN, Li YP. Thermal analysis and degradation mechanism of polyacrylate/ZnO nanocomposites. Polym Degrad Stab. 2005;87:103–110.
[45] Tao Q, Yuan J, Frost RL, et al. Effect of surfactant concentration on the stacking modes of organo-silylated layered double hydroxides. Appl Clay Sci. 2009;45:262–269.
[46] Wei M, Guo J, Shi Z, et al. Preparation and characterization of l-cystine and l-cysteine intercalated layered double hydroxides. J Mater Sci. 2007;42:2684–2689.
[47] Castro DC, Cavalcante RP, Jorge J, et al. Synthesis and characterization of mesoporous Nb_2O_5 and its application for photocatalytic degradation of the herbicide methylviologen. J Braz Chem Soc. 2016;27:303–313.
[48] Hashim N, Hussein MZ, Isa I, et al. Synthesis and controlled release of cloprop herbicides from cloprop-layered double hydroxide and cloprop-zinc-layered hydroxide nanocomposites. Open J Inorg Chem. 2014;2014:1–9.
[49] Li B, He J, Evans DG, et al. Enteric-coated layered double hydroxides as a controlled release drug delivery system. Int J Pharm. 2004;287:89–95.
[50] Tang CY, Kwon YN, Leckie JO. Probing the nano- and micro-scales of reverse osmosis membranes-A comprehensive characterization of physiochemical properties of uncoated and coated membranes by XPS, TEM, ATR-FTIR, and streaming potential measurements. J Memb Sci. 2007;287:146–156.
[51] Tyner KM, Schiffman SR, Giannelis EP. Nanobiohybrids as delivery vehicles for camptothecin. J Control Release. 2004;95:501–514.
[52] Murtaza G, Ahmad M, Shahnaz G. Microencapsulation of diclofenac sodium by non- solvent addition technique. Trop J Pharm Res. 2010;9:187–195.
[53] Kovanda F, Maryšková Z, Kovář P. Intercalation of paracetamol into the hydrotalcite-like host. J Solid State Chem. 2011;184:3329–3335.
[54] Kong X, Shi S, Han J, et al. Preparation of Glycy-l-Tyrosine intercalated layered double hydroxide film and its *in vitro* release behavior. Chem Eng J. 2010;157:598–604.
[55] Hashim N, Muda Z, Hamid SA, et al. Characterization and controlled release formulation of agrochemical herbicides based on zinc-layered hydroxide-3-(4-methoxyphenyl) propionate nanocomposite. J Phys Chem Sci. 2014;1:1–6.
[56] Nabipour H, Sadr MH, Thomas N, et al. Synthesis, characterisation and sustained release properties of layered zinc hydroxide intercalated with amoxicillin trihydrate. J Exp Nanosci. 2015;10:1269–1284.